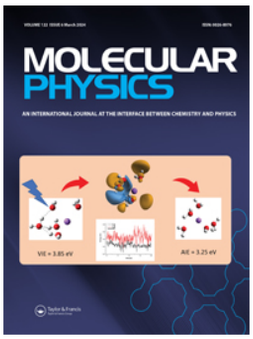

Taylor & Francis
Taylor & Francis Group

Molecular Physics

An International Journal at the Interface Between Chemistry and Physics

ISSN: (Print) (Online) Journal homepage: www.tandfonline.com/journals/tmph20

The absorption spectrum of the $H_2{}^{14}O$ radioactive isotopologue of water vapour

Boris A. Voronin, Jonathan Tennyson, Tatyana Yu. Chesnokova, Aleksei V. Chentsov & Aleksandr D. Bykov

To cite this article: Boris A. Voronin, Jonathan Tennyson, Tatyana Yu. Chesnokova, Aleksei V. Chentsov & Aleksandr D. Bykov (28 Mar 2024): The absorption spectrum of the $H_2{}^{14}O$ radioactive isotopologue of water vapour, Molecular Physics, DOI: 10.1080/00268976.2024.2333474

To link to this article: https://doi.org/10.1080/00268976.2024.2333474

Published online: 28 Mar 2024.

MOLECULAR PHYSICS e2333474
https://doi.org/10.1080/00268976.2024.2333474

Taylor & Francis
Taylor & Francis Group

FESTSCHRIFT IN HONOUR OF PROF. ATTILA G. CSÁSZÁR

The absorption spectrum of the $H_2{}^{14}O$ radioactive isotopologue of water vapour

Boris A. Voronin[a,b], Jonathan Tennyson [c], Tatyana Yu. Chesnokova[b], Aleksei V. Chentsov[b] and Aleksandr D. Bykov[b]

[a]Instituto de Fisica Gleb Wataghin, Universidade Estadual de Campinas, Campinas, Brazil; [b]V.E. Zuev Institute of Atmospheric Optics SB RAS, Tomsk, Russia; [c]Department of Physics and Astronomy, University College London, London UK

ABSTRACT

The predicted rotation-vibration absorption spectrum of the radioactive isotopically substituted water molecule, $H_2{}^{14}O$, is presented. Variational nuclear-motion calculations are performed using the DVR3D software package based on the use of a high-precision potential energy function and an accurate dipole moment surface. Line centres, intensity and Einstein coefficients are calculated, and air pressure broadening coefficients are estimated. The calculation was carried out over a wide wavenumber range from 0 to 25000 cm^{-1} and total angular momentum up to $J = 20$. Isotopologue extrapolation rules based on experimental data on the energy levels of the stable isotopologues $H_2{}^{16}O$, $H_2^{16}O$ $H_2{}^{17}O$ and $H_2{}^{18}O$ were also used to improve the predicted line positions. Spectral ranges best suited to the detection of $H_2{}^{14}O$ are identified.

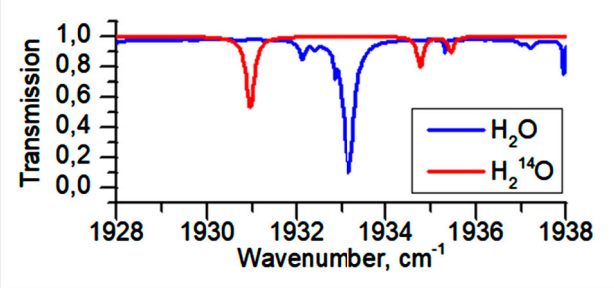

ARTICLE HISTORY
Received 8 February 2024
Accepted 6 March 2024

KEYWORDS
$H_2{}^{14}O$; energy levels; water vapour; absorption lines

1. Introduction

Water is one of the most important molecules for humans and their environment. In particular, water is molecule number one in spectroscopic data banks HITRAN [1] and GEISA [2], which emphasises its importance.

According to the NASA Extragalactic Database summary of the abundances of molecules in galaxies [3] H_2O is one of the most abundant molecules, behind only $^1H_2$, $^{12}C^{16}O$ and possibly the $^{16}O^1H$ radical. As a result, there are a large number of scientific studies on the spectroscopy of water aimed at both terrestrial and astrophysical applications. Calculated line lists for the main. parent isotopologue, $H_2{}^{16}O$, include Partridge and Schwenke [4], BT2 [5], VoTe [6,7], POKAZATEL [8] and others. There are also calculated line lists for other isotopologues, including for both stable oxygen isotopologues, $H_2{}^{17}O$ and $H_2{}^{18}O$, [9], and hydrogen isotopologues, for example, $HD^{16}O$ – VTT [10].

Radioactive isotopologues of water, such as $HT\ ^{16}O$, $T_2{}^{16}O$, have been studied both experimentally and theoretically [11,12]. Studies of radioactive isotopologues of molecules, including isotopologues of water, are of interest for many reasons. Radioactive isotopologues of atmospheric gases are formed when the Earth's atmosphere is irradiated by cosmic rays. The interaction of atmospheric molecules with cosmic rays leads, for example, to the accumulation of tritium water and the isotopologue $^{14}C^{16}O_2$ [13] in the atmosphere. It was discovered that radioactive isotopes of beryllium, carbon, nitrogen, and oxygen are produced in lightning discharges [14,15], which obviously can lead to the appearance in the atmosphere of water isotopologues $H_2{}^{14}O$ and $H_2{}^{15}O$. It was also discovered that radioactive isotopologues of water are formed when a target containing deuterium is irradiated with femtosecond laser pulses [16]. Light oxygen isotopologues of water vapour, for example $H_2{}^{15}O$ and

CONTACT Jonathan Tennyson j.tennyson@ucl.ac.uk Department of Physics and Astronomy, University College London, Gower Street, London WC1E 6BT, UK

$H_2{}^{14}O$ are actively used in medicine [17–20]. These two molecules are relatively long-lived as ^{14}O and ^{15}O have half-lives of 70.62 and 122.27 s, respectively; both isotopes decay by positron emission. The heavy oxygen radioactive isotopologue of water, $H_2{}^{19}O$, is produced by neutron irradiation of various media containing water, for example, in the primary cooling circuit of nuclear reactors [21]; ^{19}O has a half-life of 26.47 s. Here we concentrate on the light isotopologue, $H_2{}^{14}O$. This article is a continuation of our work on the spectra of oxygen short-lived radioactive isotopologues of water vapour [22–26].

The literature on $H_2{}^{14}O$ is fairly sparse. Schueller [27] did a PhD on 'Investigating $H_2{}^{14}O$ and $^{10}CO_2$ as cerebral blood flow tracers in PET' and subsequently Schueller *et al.* identified γ-ray emissions from ^{14}O (and other radioactive isotopologues) as a cause of interference in standard PET scans. $H_2{}^{14}O$ is considered in the books about radionuclides production [28–31] which are also largely concerned with medical applications.

Conversely, a technical report from Berkeley National Laboratory [32] on $H_2{}^{14}O$ production is related to astrophysics and notes the importance of this isotopologue for the physics of stars. ^{14}O oxygen is known to be important for understanding the physics of stars [33–37], and, of course, stars are largely composed of hydrogen.

It is significantly easier to calculate the spectrum of $H_2{}^{14}O$ using a method of proven accuracy than to measure it. In this paper, we present the theoretical infrared absorption spectrum of $H_2{}^{14}O$ for the first time.

2. Calculated spectrum of $H_2{}^{14}O$

We present a theoretical absorption spectrum of $H_2{}^{14}O$ obtained via direct variational calculation of line centres and intensities involving rotation states up to $J = 20$ using a high accuracy potential energy surface (PES) from [38], and a dipole moment surface (DMS) from [39]. The calculations were carried out as follows. At the first stage of the calculation, the vibrational-rotational (VR) energy levels and wave functions were calculated. The energy levels of $H_2{}^{14}O$ were calculated using the variational nuclear-motion program DVR3D [40]. Previous studies have shown that DVR3D gives highly converged results for vibration-rotation levels of water [41].

The energy levels of $H_2{}^{14}O$ were calculated in the same way as for the parent isotopologue $H_2{}^{16}O$, except that the mass of the oxygen atom was set to mass 14.008596706 [42]. The calculations were carried out on the 'amun' cluster (at UCL) and on computers of the Gleb Watagin Institute of Physics (IFGW, Campinas, Brazil).

Table 1 lists the names of the files that form the basis for calculating the spectrum of $H_2{}^{14}O$. These are 12 files with transitions consisting of 3 columns (see Table 3). For all files in Table 1, their name and size are indicated. Transition files contain a range and number of transitions. There are more than 106 500 000 transition in total. This procedure has been used to produce a number of line list for H_2O and it isotopologues including BT2 [40], VTT [10], POKAZATEL [8], Conway [43], HotWat78 [9] and VoTe [6,7].

Table 1. Contents of the directory with files for calculating $H_2{}^{14}O$.

File name	N. trans./lines	Size, Mb	Range,cm^{-1}
00000-00500-VoTe14.txt	7 255 008	177	0-500
00500-01000-VoTe14.txt	6 977 348	170	500-1000
01000-01500-VoTe14.txt	6 659 198	162	1000-1500
01500-02000-VoTe14.txt	6 313 310	154	1500-2000
02000-02500-VoTe14.txt	5 956 980	145	2000-2500
02500-03500-VoTe14.txt	10 963 500	268	2500-3500
03500-04500-VoTe14.txt	9 699 037	237	3500-4500
04500-05500-VoTe14.txt	8 539 226	209	4500-5500
05500-07000-VoTe14.txt	10 859 543	266	5500-7000
07000-09000-VoTe14.txt	11 250 131	275	7000-9000
09000-14000-VoTe14.txt	15 981 824	392	9000-14000
14000-25000-VoTe14.txt	6 223 558	153	14000-25000
energy-levelsH214O-N.dat	72 920	4	0-26000
H214O-spectrum-296K.dat	251 560	30.7	0-25000

3. Line list

The line list for $H_2{}^{14}O$, which we call VoTe-14, designed for use at room temperature over a wide range of wavenumbers has been constructed. It contains 72 920 states and 106 678 663 (more than one hundred million) transitions in total. The $H_2{}^{14}O$ (VoTe-14) line list is available from the ExoMol database www.exomol.com using the standard ExoMol format [44]. Extracts from the States `.states` and Transition `.trans` files are shown in Tables 2 and 3, respectively. The State file contains a list of ro-vibrational states of $H_2{}^{14}O$ with the state ID numbers, energy term values (in cm^{-1}), uncertainties (in cm^{-1}) and quantum numbers: the provision of which are discussed below. The exact quantum numbers are the total angular momentum J and the total symmetry $\Gamma = A_1, A_2, B_1, B_2$ in the Molecular Symmetry group $C_{2v}(M)$. The total state degeneracy, g_i is given by $(2J+1)$ times the nuclear spin factor, g_{ns}. For $H_2{}^{14}O$ the nuclear spins g_{ns} are 1, 1, 3, and 3 for $\Gamma = A_1, A_2, B_1, B_2$, respectively, like $H_2{}^{16}O$ as the nuclear spin of ^{14}O is zero, which is the same as ^{16}O; both isotopologues therefore have ortho and para states with a degeneracy ratio 3:1.

In addition, for some of the levels, approximate quantum numbers in the traditional rotation-vibrational identification v_1, v_2, v_3, K_a, K_c are also given; the provision of these is discussed below. Here v_1, v_2, v_3 are the normal mode vibrational quantum numbers, J is the (total) rotational angular momentum quantum number, K_a and

Table 2. Extract from the `.states` file of the $H_2{}^{14}O$ line list.

i	$\tilde{E}$/cm^{-1}	g	J	δ/cm^{-1}	v_1	v_2	v_3	J	K_a	K_c	e/o	Γ_{tot}	$\tilde{E}_D$/cm^{-1}	Code
1	0.000000	1	0	0.000001	0	0	0	0	0	0	e	A1	0.000000	IE
2	1602.821045	1	0	0.045795	0	1	0	0	0	0	e	A1	1602.837581	IE
3	3167.321571	1	0	0.090495	0	2	0	0	0	0	e	A1	3167.326643	IE
4	3666.422145	1	0	0.104754	1	0	0	0	0	0	e	A1	3666.383739	IE
5	4689.622895	1	0	0.133989	0	3	0	0	0	0	e	A1	4689.622895	Ca
6	5252.281862	1	0	0.150065	1	1	0	0	0	0	e	A1	5252.272096	IE
7	6163.419503	1	0	0.176098	0	4	0	0	0	0	e	A1	6163.425364	IE
8	6799.706827	1	0	0.194277	1	2	0	0	0	0	e	A1	6799.694842	IE
9	7221.260928	1	0	0.206322	2	0	0	0	0	0	e	A1	7221.258391	IE
10	7478.441757	1	0	0.213669	0	0	2	0	0	0	e	A1	7478.418449	IE
11	7577.520257	1	0	0.216501	0	5	0	0	0	0	e	A1	7577.520257	Ca
12	8305.259095	1	0	0.237293	1	3	0	0	0	0	e	A1	8305.261217	IE
13	8789.283858	1	0	0.251123	2	1	0	0	0	0	e	A1	8789.287707	IE
14	8909.428011	1	0	0.254555	0	6	0	0	0	0	e	A1	8909.428011	Ca
15	9041.330586	1	0	0.258323	0	1	2	0	0	0	e	A1	9041.311577	IE
16	9761.281946	1	0	0.278894	1	4	0	0	0	0	e	A1	9761.281946	Ca
17	10128.471339	1	0	0.289385	0	7	0	0	0	0	e	A1	10128.471339	Ca
18	10319.194475	1	0	0.294834	2	2	0	0	0	0	e	A1	10319.194475	Ca
19	10570.285795	1	0	0.302008	0	2	2	0	0	0	e	A1	10570.285795	Ca
20	10632.017432	1	0	0.303772	3	0	0	0	0	0	e	A1	10632.017432	Ca

i: state identifier;
$\tilde{E}$: state term value, DVR3D or pseudo-experimental;
g: state degeneracy;
J: state rotational quantum number;
δ: energy uncertainty;
$v_1 - v_3$: normal mode vibrational quantum numbers;
J: state rotational quantum number;
K_a and K_c: state oblate and prolate quantum numbers;
e/o even or odd – K_c: state oblate and prolate quantum numbers;
Γ_{tot}: total symmetry in C_{2v}(M).
$\tilde{E}_D$: state term value, DVR3D;
Code – Ca (Calculated by DVR3D) or IE – Isotop. Energy (Pseudo-experimental)

Table 3. Extract from a `.trans` file of the $H_2{}^{14}O$ line list.

f	i	A_{fi}
13766	12819	0.15255E−23
53440	54679	0.24241E−20
44313	45564	0.27545E−19
65810	64651	0.16649E−22
7855	9940	0.39264E−23
39054	40169	0.77269E−20
15620	18394	0.24741E−20
54811	53562	0.13271E−17
36207	39673	0.51857E−20
14613	15385	0.43321E−17
38609	37345	0.51053E−17

f: Upper state counting number;
i: Lower state counting number;
A_{fi}: Einstein-A coefficient (in s^{-1}).

K_c are the oblate and prolate rotational quantum numbers (projection of the angular momentum on the corresponding molecular axis a and c, respectively).

DVR3D only supplies rigorous quantum numbers which for H_2O correspond to J, parity and whether the state is ortho or para. To provide the approximate rotation and vibration quantum labels, namely v_1, v_2, v_3, K_a and K_c, we matched the $H_2{}^{14}O$ energies to the assigned states of the parent isotopologue $H_2{}^{16}O$ as provided in the VoTe line list [6,7], which was based on calculations with the same PES. Following VoTe, we also provide the parity of the K_c quantum number, which can be reconstructed from the (rigorous) values of J and the total symmetry Γ as shown in Table 12-7 of [45]. Here we adopt the ExoMol [46] standard and assign the value 'NaN' to the undetermined values of the quantum numbers.

As an attempt to improve the predicted energy levels of $H_2{}^{14}O$, we apply the isotopologue extrapolation (IE) corrections given Equation (1) to the set of 3426 energy levels. These states are indicated with the label 'IE' in contrast to all other, calculated values which are labelled with 'Ca'.

Following the IE or pseudo-experimental extrapolation method proposed in [9], here we use the obs.-calc. residuals for the main isotopologue to obtain empirical corrections to the ro-vibrational energy values of the minor isotopologues of water as follows :

$$E_N^{\rm corr} = E_N^{\rm calc} + E_{16}^{\rm obs} - E_{16}^{\rm calc}, \qquad (1)$$

where $E_N^{\rm calc}$ is a DVR3D energy calculated for a minor isotopologue, $N = 14$, 17, 18, and $E_{16}^{\rm obs} - E_{16}^{\rm cacl}$ is an empirical correction estimated as the difference between the calculated and experimental energies of the parent (16) molecule. The approach is based on the assumption that the main source of the error is from the inaccuracy of the Born-Oppenheimer PES of water, which should affect all four isotopologues similarly and has been shown to work well for $H_2{}^{18}O$ and $H_2{}^{17}O$ [9]. Following [9], we will refer

to $E_{16}^{\rm obs} - E_{16}^{\rm cacl}$ as the pseudo-experimental correction $E_N^{\rm corr}$.

The provision of uncertainties in the energy levels is now a formal part of the ExoMol data structure [46]. For the pseudo-experimental values, the uncertainties are estimated as the the obs.-calc. residuals of the $H_2{}^{16}O$ isotopologue obtained as the difference between the W2020 and DVR3D energy values.

For this work, the following, slightly less conservative formula (2) was used, which gives similar results (in cm^{-1}):

$$\text{unc} = \Delta\xi\tilde{E} + \Delta BJ(J+1), \tag{2}$$

at our case $\Delta\xi = 1/35000$ cm^{-1} and $\Delta B = 0.0005$ cm^{-1}. This formula 2 was obtained via correlation and autocorrelation methods [47] applied to the W2020 [48] data of the three isotopologues in conjunction with the method of [49].

We can take the uncertainties for 19225 $H_2{}^{16}O$ levels from W2020, and calculate the errors using the formula in (2). For rotational-vibrational states, where the energies of all three $H_2{}^{16}O$ isotopologues were present in W2020, we doubled the uncertainty of the main isotopologues, since it is very small. 3426 levels were replaced by the pseudo-experimental values. The maximum differences of these changes do not exceed 0.1 cm^{-1}.

The $H_2{}^{14}O$ `.trans` files contain Einstein A coefficients (in s^{-1}) together with the upper and lower state ID numbers. To stop the files from being inconveniently large, the transitions are divided into twelve Transition files according the the following spectroscopic ranges: 0-500, 500-1000, 1000-1500, 1500-2000, 2000-2500, 2500-3500, 3500-4500, 4500-5500, 5500-7000, 7000-9000, 9000-14000, 14000-25000 cm^{-1}.

4. Partition function, $Q(T)$, for $H_2{}^{14}O$ as a function of temperature, T(K).

Using vibrational-rotational energy levels, the partition function of $H_2{}^{14}O$ was calculated for different temperatures up to 1000 K using

$$Q(T) = \sum_i g_i \exp\left(-\frac{E_i}{kT}\right). \tag{3}$$

It is included as part of our supplementary material. The file format is quite simple, two columns with the temperature in K and $Q(T)$.

Figure 1 shows a comparison of partition functions $Q(T)$ of the $H_2{}^{14}O$, $H_2{}^{16}O$ and $H_2{}^{15}O$ species for the temperature range from 1 to 1000 K. The main difference is the nuclear spin factor, which is 2 times larger for $H_2{}^{15}O$ as ^{15}O has $I = \frac{1}{2}$. As noted above, for $H_2{}^{14}O$ the nuclear spins $g_{\rm ns}$ are 1, 1, 3, and 3 for A_1, A_2, B_1, B_2, respectively. This $H_2{}^{14}O$ linelist can be used to generate spectra with different temperatures up to 1000 K. To generate converged $H_2{}^{14}O$ spectra at higher temperatures

Table 4. Examples spectrum for applications.

C.	w.n.cm^{-1}	Intensity	A.coeff.	G_{air}	G_{self}	E_{low}	k_{Td}	shift	$v_1' v_2' v_3'$	$J' K_a' K_c'$	$v_1\ v_2\ v_3$	$J\ K_a K_c$
10	0.261084	0.275E−28	0.257E−09	0.0870	0.523	1932.704023	0.69	0.0	0 1 0	4 2 2	0 1 0	5 1 5
10	1.408154	0.172E−23	0.148E−07	0.0746	0.443	448.226751	0.69	0.0	−2 -2 -2	6 -2 -2	0 0 0	5 2 3
10	1.567057	0.594E−26	0.674E−07	0.0870	0.523	1829.424296	0.77	0.0	0 1 0	4 1 4	0 1 0	3 2 1
10	1.601197	0.361E−26	0.830E−07	0.0925	0.563	1918.552160	0.73	0.0	0 1 0	3 3 0	0 1 0	4 2 3
10	2.156354	0.572E−28	0.759E−07	0.0471	0.290	2917.184407	0.49	0.0	0 1 0	10 2 9	0 1 0	9 3 6
10	2.301379	0.225E−26	0.172E−06	0.0870	0.523	2143.120228	0.69	0.0	0 1 0	4 4 1	0 1 0	5 3 2
10	2.336767	0.139E−29	0.422E−06	0.0870	0.523	3617.357190	0.69	0.0	0 2 0	4 3 1	0 2 0	5 2 4
10	2.847266	0.337E−28	0.111E−06	0.0284	0.207	2887.104031	0.36	0.0	0 0 0	14 4 10	0 0 0	15 3 13
10	5.055372	0.224E−25	0.301E−05	0.0989	0.478	1748.518606	0.77	0.0	0 1 0	2 2 0	0 1 0	3 1 3
10	5.254574	0.587E−22	0.234E−05	0.0925	0.563	137.917800	0.78	0.0	−2 -2 -2	3 -2 -2	0 0 0	2 2 0
10	5.638201	0.202E−29	0.943E−06	0.0153	0.160	4028.796338	0.38	0.0	0 0 0	17 4 13	0 0 0	16 7 10
10	5.685129	0.125E−29	0.292E−05	0.0925	0.563	3801.071980	0.78	0.0	1 0 0	3 1 3	1 0 0	2 2 0
10	6.136196	0.529E−26	0.322E−05	0.0870	0.523	2139.302888	0.69	0.0	0 1 0	4 4 0	0 1 0	5 3 3
10	7.216464	0.105E−28	0.100E−04	0.0808	0.495	3886.479812	0.64	0.0	0 2 0	5 4 1	0 2 0	6 3 4
10	7.372747	0.116E−28	0.871E−05	0.0925	0.563	3514.002088	0.73	0.0	0 2 0	3 3 1	0 2 0	4 2 2
10	7.681668	0.195E−28	0.257E−05	0.0232	0.198	3453.394301	0.38	0.0	0 0 0	15 6 10	0 0 0	16 3 13

C. 10-code-molecule number+isotopologue number;
Transition wavenumber, cm^{-1};
Line Intensity at 100% abundance, cm/molecule ;
Einstein A-coefficient;
Air- broadened width, cm^{-1}/atm;
Self- broadened width, cm^{-1}/atm;
lower-state Energy, cm^{-1};
Temperature dependence (of air width), unitless;
Pressure shift, always zero in our case;
upper vibrational quanta, v_1', v_2', v_3';
upper local quanta, J', K_a', K_c';
lower vibrational quanta, v_1, v_2, v_3;
lower local quanta, J, K_a, K_c.

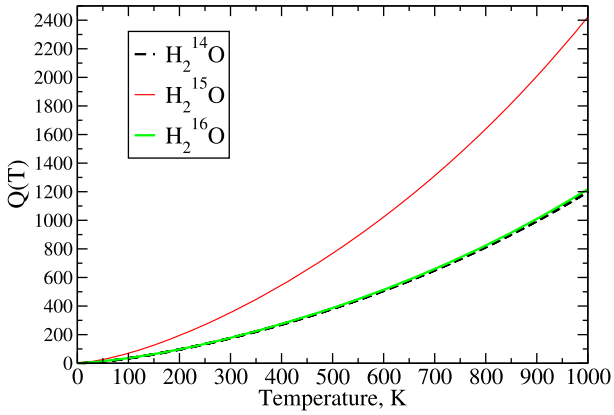

Figure 1. Partition function $Q(T)$ for $H_2{}^{14}O$, $H_2{}^{15}O$ and $H_2{}^{16}O$ water for temperature range from 1 to 1000 K.

will require additional calculations. For more details, see papers [50,51]. A file tabulating our partition function (PartFunc-H214O.dat) is given as Supplementary Data.

5. Spectrum of $H_2{}^{14}O$ for applications

The line list produced was used to model spectra of $H_2{}^{14}O$.

A room temperature $H_2{}^{14}O$ line list (296 K) was generated using the intensity threshold of $> 10^{-30}$ cm/molecule for atmospheric applications. It contains 251560 lines using the format similar to that of HITRAN2020 [1], see Table 4 and is provided as part of the supplementary material.

The HITRAN database provides data for seven isotopologues of water using the following isotopologue codes: 11 ($H_2{}^{16}O$), 12 ($H_2{}^{18}O$), 13 ($H_2{}^{17}O$), 14($HD^{16}O$), 15($HD^{18}O$), 16($HD^{17}O$), 17($D_2{}^{16}O$). We adopted 18 as a code for $H_2{}^{15}O$ [26] since this number is not yet taken in HITRAN and suggest 10 for $H_2{}^{14}O$, keeping 19 for $H_2{}^{19}O$. The line list consists of the isotopologue code (10) (Molecule number 1 + Isotopologue number 0), line positions, 296 K intensities (cm/molecule), Einstein coefficients (s^{-1}), air-broadened widths (γ_{air}, cm^{-1}/atm), self-broadened widths (γ_{self}, cm^{-1}/atm), temperature dependence component of air n_{air}, line shifts (set to 0.0 cm^{-1}) and ro-vibrational quantum number (Table 5). The line-broadening parameters were evaluated using the J and 'JJ—dependency' methods [52]. For the temperature-dependence exponent n_{air} (unitless) we assumed the water vapour air-broadened half-widths from Table 7 of HITRAN2004 [53].

6. Energy levels for $H_2{}^{14}O$, $H_2{}^{15}O$ and $H_2{}^{16}O$

For some applications, it is convenient when there is a correlation of the same energy levels of different isotopic modifications. This can be useful for both identification and extrapolation and comparison problems. In view of this, we offer the reader Table 6, which is fully presented in additional materials. The table shows the quantum identification and symmetry and energy levels for $H_2{}^{14}O$, $H_2{}^{15}O$ and $H_2{}^{16}O$.

$H_2{}^{15}O$ energy levels were taken from [26] and $H_2{}^{16}O$ levels from [7]. The rigorous quantum numbers J, s and N were used to uniquely identify each level, where J is the rotational quantum number, $s = 1, 2, 3$ and 4 denotes overall symmetry A_1, A_2, B_1 and B_2, respectively and N is a counting number with each (J,s) subset. Table 6 also gives v_1, v_2, v_3 – normal mode vibrational quantum numbers; J – state rotational quantum number; K_a and K_c: state oblate and prolate quantum numbers where possible. Energy levels were calculated using a set

Table 5. Partition function, $Q(T)$, for $H_2^{14}O$ as a function of temperature, T, in K.

T	$Q(T)$	T	$Q(T)$	T	$Q(T)$	T	$Q(T)$
1	1.000	287	164.961	309	184.220	375	246.393
20	3.319	288	165.821	310	185.113	380	251.369
40	9.323	289	166.681	311	186.007	385	256.382
60	16.648	290	167.544	312	186.903	390	261.431
85	27.477	291	168.407	313	187.801	395	266.519
110	39.979	292	169.273	314	188.700	400	271.643
135	53.968	293	170.140	315	189.601	405	276.805
160	69.305	294	171.008	316	190.503	410	282.003
185	85.887	295	171.878	317	191.407	435	308.557
210	103.631	296	172.750	318	192.312	460	336.047
235	122.472	297	173.623	319	193.219	485	364.480
260	142.357	298	174.497	320	194.127	510	393.863
265	146.456	299	175.374	325	198.691	535	424.206
270	150.595	300	176.251	330	203.292	560	455.518
275	154.773	301	177.131	335	207.932	585	487.808
280	158.991	302	178.011	340	212.608	610	521.087
281	159.839	303	178.894	345	217.323	635	555.364
282	160.689	304	179.778	350	222.075	660	590.649
283	161.540	305	180.663	355	226.864	685	626.952
284	162.393	306	181.550	360	231.690	690	634.336
285	163.248	307	182.438	365	236.554	695	641.761
286	164.104	308	183.328	370	241.455	700	649.227

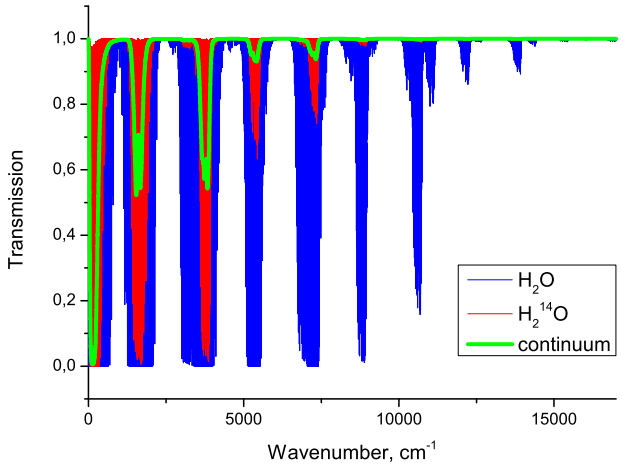

Figure 2. Transmission spectra of H_2O, $H_2{}^{14}O$ and H_2O continuum. The $H_2{}^{14}O/H_2O$ ratio is 0.5%.

Table 6. Energy levels for $H_2{}^{14}O$, $H_2{}^{15}O$ and $H_2{}^{16}O$ in cm^{-1}, see text for a discussion of the quantum numbers.

J	s	N	v_1	v_2	v_3	J	K_a	K_c	E_{14}	E_{15}	E_{16}
0	1	1	0	0	0	0	0	0	0.000000	0.000000	0.000000
0	1	2	0	1	0	0	0	0	1602.837581	1598.538460	1594.762713
0	1	3	0	2	0	0	0	0	3167.326643	3158.973045	3151.635009
0	4	1	0	0	1	0	0	0	3774.067258	3764.382357	3755.932087
0	4	2	0	1	1	0	0	0	5357.433521	5343.474407	5331.267334
0	4	3	0	2	1	0	0	0	6905.287692	6887.277773	6871.508312
1	2	269	−2	−2	−2	1	−2	1	25998.618178	25949.737841	25907.494127
1	2	270	0	13	2	1	1	1	26051.794471	26003.859527	25951.750492
1	2	271	−2	−2	−2	1	−2	1	26068.240543	26012.475229	25964.087973
1	2	272	3	6	2	1	1	1	26080.749405	26014.963603	25967.452834
1	3	273	−2	−2	−2	1	−2	1	26082.331339	26032.004480	25988.351431
1	3	274	−2	−2	−2	1	−2	1	26139.137771	26080.016130	26011.515390
2	4	374	0	8	4	2	1	2	25901.208886	25850.872882	25803.973642
2	4	375	1	1	6	2	1	2	25923.959264	25859.970069	25807.278270
2	4	376	−2	−2	−2	2	−2	−88	25941.478091	25882.827376	25831.593544
2	4	377	1	15	0	2	1	2	25983.687339	25915.150753	25854.439531
4	2	508	−2	−2	−2	4	−2	−77	26048.800918	25992.268321	25939.727194
4	2	509	0	3	6	4	3	1	26064.699210	25995.462784	25942.760685
4	2	510	1	1	6	4	1	3	26085.545757	26034.754065	25990.654539
4	2	511	−2	−2	−2	4	−2	−77	26105.576003	26045.832935	25993.592149
4	2	512	−2	−2	−2	4	−2	−77	26120.699892	26066.427794	26012.800593
4	2	513	−2	−2	−2	4	−2	−77	26129.910934	26067.453374	26018.990910

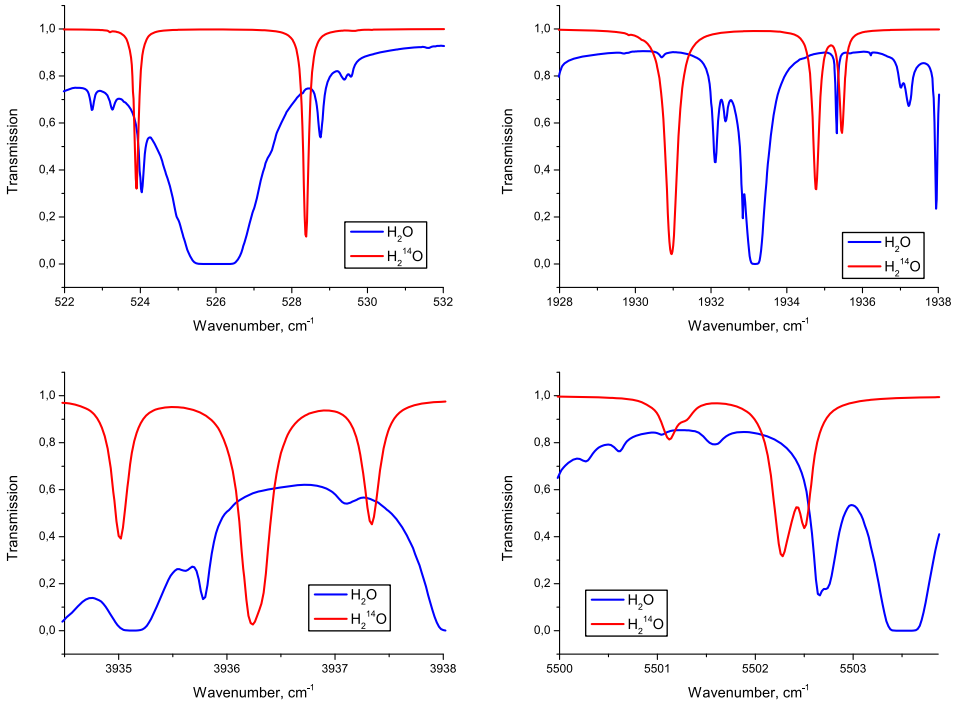

Figure 3. Prospective spectral windows for the $H_2{}^{14}O$ detection. The air pressure is 1 atm; the H_2O partial pressure is 18800 ppm; the temperature is 294 K. The path length is 100 m. The $H_2{}^{14}O/H_2O$ ratio is 0.5%.

of parameters for all isotopologues except for the oxygen mass. It should be noted that $E_{14} > E_{15} > E_{16}$ for all levels except the lowest which is set to zero by convention.

7. Simulation of $H_2{}^{14}O$ transmission for laboratory conditions

To find the prospective spectral regions for the $H_2{}^{14}O$ detection, we have simulated the H_2O transmission spectra with varying of $H_2{}^{14}O$ concentration. The calculations were made using line-by-line method [54] with a spectral resolution of 0.02 cm^{-1} for laboratory conditions with air pressure of 1 atm, H_2O partial pressure of 18800 ppm and temperature of 294 K. The paths with length of 100 m and 20 m were considered. The transmission spectra of H_2O, $H_2{}^{14}O$ and H_2O continuum in the 0-20000 cm^{-1} region are shown in Figure 2. The spectrum of H_2O includes absorption by spectral lines of main isotopologues of H_2O ($H_2{}^{16}O$, $H_2{}^{18}O$, $H_2{}^{17}O$, $HD^{16}O$, $HD^{18}O$, $HD^{17}O$) from

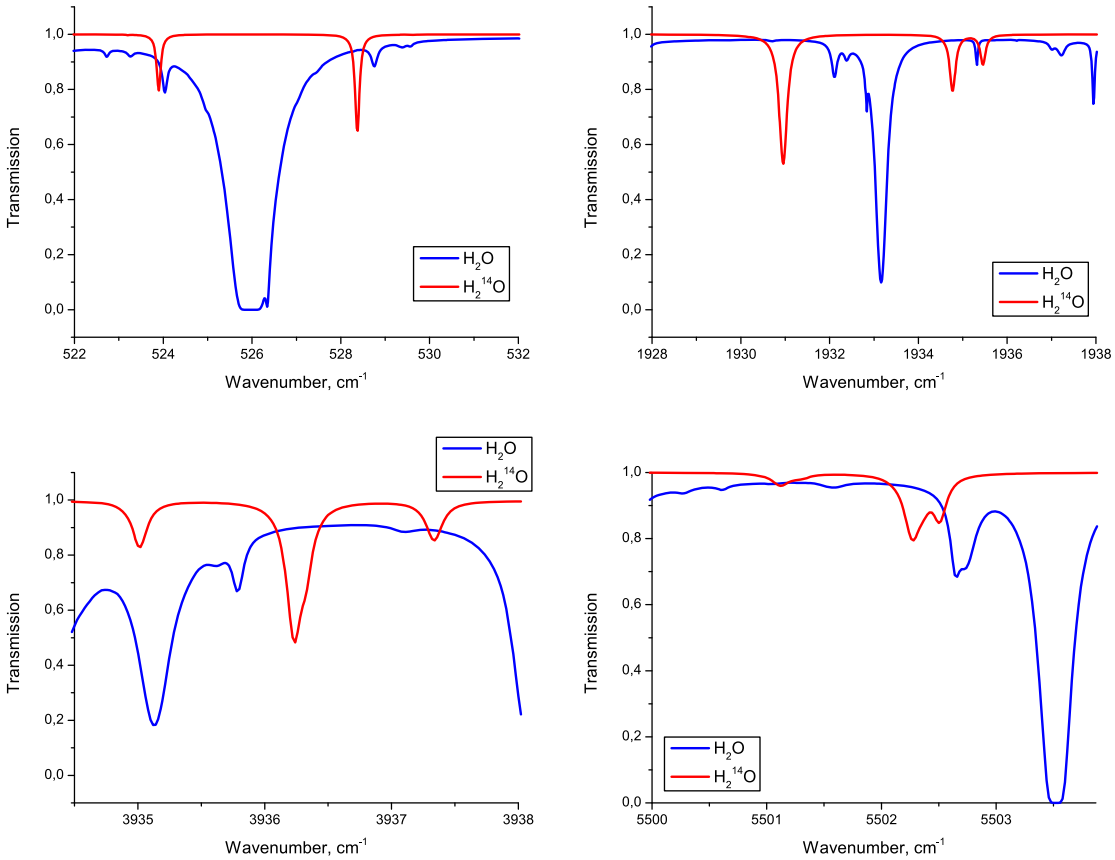

Figure 4. Perspective spectral windows for the $H_2{}^{14}O$ detection. The air pressure is 1 atm; the H_2O partial pressure is 18800 ppm; the temperature is 294 K. The path length is 20 m. The $H_2{}^{14}O/H_2O$ ratio is 0.5%.

the HITRAN2020 spectroscopic database [1] in natural abundance. The H_2O continuum was calculated using the MT_CKD model [55]. The transmission simulation used our computed $H_2{}^{14}O$ lines parameters, such as position and intensity of the line, lower-state energy of the transition, air-broadened and self-broadened half-widths, air pressure-induced line shift, and temperature-dependence exponent for air-broadened half-width. It was found that a ratio of $H_2{}^{14}O$ to H_2O in natural abundance of more than 0.5% should allow $H_2{}^{14}O$ to be detected by high-resolution spectrometers in laboratory conditions. The spectral windows suitable for detection of $H_2{}^{14}O$ are shown in Figures 3 and 4. The perspective windows lie in the IR and NIR regions: 522-532 cm^{-1}, 1928-1938 cm^{-1}, 3934-3938 cm^{-1} and 5500-5503 cm^{-1}.

8. Conclusions

The authors hope that the predicted spectrum of $H_2{}^{14}O$ will be a useful tool for PET tomography, astrophysics and plasma chemistry and aid the detection of this isotopologue. It can be assumed that $H_2{}^{14}O$ water plays a greater role in fast-paced complex chemical and nuclear processes than previously assumed. This is primarily due to the fact that the previously a calculated IR spectrum $H_2{}^{14}O$ simply did not exist.

Acknowledgments

The authors thank Prof. S.N. Yurchenko for useful consultations and Prof. Flávio C. Cruz for partially funding this work. *Boris A. Voronin*: Term, Validation, Investigation, Writing – Original Draft; *Jonathan Tennyson*: Supervision, Conceptualisation, Resources, Writing – Review & Editing, Methodology; *Tatyana Yu. Chesnokova*: Investigation, Data Curation, Writing – Review & Editing; *Aleksei V. Chentsov*: Formal analysis, Visualisation; *Aleksandr D. Bykov*: Conceptualisation, Validation.

Data availability statement

The line list is provided via the ExoMol website www.exomol.com. File `PartFunc-H214O.dat` containing only 2 columns, can be found in the supplementary materials. In the first column, the temperature in K, from 1 to 1000 K, in the second column, the value of the partition function for a given temperature. File H214O-spectrum-296K.dat as at Table (4) can be found in the supplementary materials. At https://ftp.iao.ru/pub/VTT/H214O/, the explanation and notation for the file with atmospheric/laboratory application are provided. Some other files and data are available from the same internet link. The file format for laboratory applications

available is presented in Table 4. Any questions about the data can be directed to Boris Voronin and Jonathan Tennyson.

Disclosure statement

No potential conflict of interest was reported by the author(s).

Funding

Boris Voronin is grateful for the financial support of the grant – FAPESP (2022/08772-1). The work was partially supported by the MSHE RF (V.E. Zuev IAO SB RAS) and NERC grant NE/F01967X/1.

ORCID

Jonathan Tennyson http://orcid.org/0000-0002-4994-5238

References

[1] I.E. Gordon, L.S. Rothman, R.J. Hargreaves, R. Hashemi, E.V. Karlovets, F.M. Skinner, E.K. Conway, C. Hill, R.V. Kochanov, Y. Tan, P. Wcisło, A.A. Finenko, K. Nelson, P.F. Bernath, M. Birk, V. Boudon, A. Campargue, K.V. Chance, A. Coustenis, B.J. Drouin, J.-M. Flaud, R.R. Gamache, J.T. Hodges, D. Jacquemart, E.J. Mlawer, A.V. Nikitin, V.I. Perevalov, M. Rotger, J. Tennyson, G.C. Toon, H. Tran, V.G. Tyuterev, E.M. Adkins, A. Baker, A. Barbe, E. Canè, A.G. Császár, A. Dudaryonok, O. Egorov, A.J. Fleisher, H. Fleurbaey, A. Foltynowicz, T. Furtenbacher, J.J. Harrison, J.-M. Hartmann, V.-M. Horneman, X. Huang, T. Karman, J. Karns, S. Kassi, I. Kleiner, V. Kofman, F. Kwabia–Tchana, N.N. Lavrentieva, T.J. Lee, D.A. Long, A.A. Lukashevskaya, O.M. Lyulin, V.Y. Makhnev, W. Matt, S.T. Massie, M. Melosso, S.N. Mikhailenko, D. Mondelain, H.S.P. Müller, O.V. Naumenko, A. Perrin, O.L. Polyansky, E. Raddaoui, P.L. Raston, Z.D. Reed, M. Rey, C. Richard, R. Tóbiás, I. Sadiek, D.W. Schwenke, E. Starikova, K. Sung, F. Tamassia, S.A. Tashkun, J. Vander Auwera, I.A. Vasilenko, A.A. Vigasin, G.L. Villanueva, B. Vispoel, G. Wagner, A. Yachmenev and S.N. Yurchenko, J. Quant. Spectrosc. Radiat. Transf. **277**, 107949 (2022). doi:10.1016/j.jqsrt.2021.107949

[2] N. Jacquinet-Husson, R. Armante, N.A. Scott, A. Chédin, L. Crépeau, C. Boutammine, A. Bouhdaoui, C. Crevoisier, V. Capelle, C. Boonne, N. Poulet-Crovisier, A. Barbe, D.C. Benner, V. Boudon, L.R. Brown, J. Buldyreva, A. Campargue, L.H. Coudert, V.M. Devi, M.J. Down, B.J. Drouin, A. Fayt, C. Fittschen, J.-M. Flaud, R.R. Gamache, J.J. Harrison, C. Hill, Ø. Hodnebrog, S.M. Hu, D. Jacquemart, A. Jolly, E. Jiménez, N.N. Lavrentieva, A.W. Liu, L. Lodi, O.M. Lyulin, S.T. Massie, S. Mikhailenko, H.S.P. Müller, O.V. Naumenko, A. Nikitin, C.J. Nielsen, J. Orphal, V.I. Perevalov, A. Perrin, E. Polovtseva, A. Predoi-Cross, M. Rotger, A.A. Ruth, S.S. Yu, K. Sung, S.A. Tashkun, J. Tennyson, .G. Tyuterev, J. Vander Auwera, B.A. Voronin and A. Makie, J. Mol. Spectrosc. **327**, 31–72 (2016). doi:10.1016/j.jms.2016.06.007

[3] B.F. Madore, LEVEL 5: A Knowledgebase for Extragalactic Astronomy and Cosmology, Tech. rep., NASA. https://ned.ipac.caltech.edu/level5/ (2020).

[4] H. Partridge and D.W. Schwenke, J. Chem. Phys. **106** (11), 4618–4639 (1997). doi:10.1063/1.473987

[5] R.J. Barber, J. Tennyson, G.J. Harris and R.N. Tolchenov, Mon. Not. R. Astron. Soc. **368** (3), 1087–1094 (2006). doi:10.1111/j.1365-2966.2006.10184.x

[6] B.A. Voronin, J. Tennyson and L. Lodi, The VoTe room temperature $H_2^{16}O$ line list up to 25000 cm^{-1}, in 24th International Symposium on Atmospheric and Ocean Optics: Atmospheric Physics, Vol. 10833, 2018, pp. 10833H.

[7] B.A. Voronin, J. Tennyson, L. Lodi and A. Kozodoev, Opt. Spectrosc. **127** (6), 967–973 (2019). doi:10.1134/S0030400X19120397

[8] O.L. Polyansky, A.A. Kyuberis, N.F. Zobov, J. Tennyson, S.N. Yurchenko and L. Lodi, Mon. Not. R. Astron. Soc. **480** (2), 2597–2608 (2018). doi:10.1093/mnras/sty1877

[9] O.L. Polyansky, A.A. Kyuberis, L. Lodi, J. Tennyson, R.I. Ovsyannikov and N. Zobov, Mon. Not. R. Astron. Soc. **466** (2), 1363–1371 (2017). doi:10.1093/mnras/stw3125

[10] B.A. Voronin, J. Tennyson, R.N. Tolchenov, A.A. Lugovskoy and S.N. Yurchenko, Mon. Not. R. Astron. Soc. **402** (1), 492–496 (2010). doi:10.1111/j.1365-2966.2009.15904.x

[11] M.J. Down, J. Tennyson, M. Hara, Y. Hatano and K. Kobayashi, J. Mol. Spectrosc. **289**, 35–40 (2013). doi:10.1016/j.jms.2013.05.016

[12] V. Hermann, A. Freise, M. Schlösser, F. Hase and J. Orphal, JMS. **398**, 111859 (2023).

[13] J.-C. David and I. Leya, Prog. Part. Nucl. Phys. **109**, 103711 (2019). doi:10.1016/j.ppnp.2019.103711

[14] L.P. Babich, Phys. Usp. **62** (10), 976–999 (2019). doi:10.3367/UFNe.2018.12.038501

[15] P.G. Ortega, J. Atmos. Sol-Terr. Phys. **208**, 105349 (2020). doi:10.1016/j.jastp.2020.105349

[16] K. Nemoto, A. Maksimchuk, S. Banerjee, K. Flippo, G. Mourou, D. Umstadter and V.Y. Bychenkov, Appl. Phys. Lett. **78** (5), 595–597 (2001). doi:10.1063/1.1343845

[17] P.T. Fox, M.A. Mintun, M.E. Raichle and P. Herscovitch, J. Cereb. Blood Flow Metab. **4** (3), 329–333 (1984). doi:10.1038/jcbfm.1984.49pMID: 6470051.

[18] A.M. Speer, M.W. Willis, P. Herscovitch, M. Daube-Witherspoon, J. Repella Shelton, B.E. Benson, R.M. Post and E.M. Wassermann, Biol. Psychiatry **54** (8), 818–825 (2003). doi:10.1016/S0006-3223(03)00002-7

[19] C.S. Carter, M. Mintun and J.D. Cohen, NeuroImage **2** (4), 264–272 (1995). doi:10.1006/nimg.1995.1034

[20] M. Kano, S. Fukudo, J. Gyoba, M. Kamachi, M. Tagawa, H. Mochizuki, M. Itoh, M. Hongo and K. Yanai, Brain **126** (6), 1474–1484 (2003). doi:10.1093/brain/awg131

[21] A. Žohar and L. Snoj, Prog. Nucl. Energy **117**, 103042 (2019). doi:10.1016/j.pnucene.2019.103042

[22] B.A. Voronin, M.V. Makarova, A.V. Poberovskii, A.D. Bykov, E.A. Dudnikiva and J. Tennyson, J. Quant. Spectrosc. Radiat. Transf **276**, 107929 (2021). doi:10.1016/j.jqsrt.2021.107929

[23] B.A. Voronin and A.D. Bykov, Proc. SPIE **11916**, 1191605 (2021).

[24] A.D. Bykov and B.A. Voronin, Atmos. Ocean. Opt. **36** (5), 339–345 (2023).

[25] B.A. Voronin, J. Tennyson, S.N. Yurchenko, T.Y. Chesnokova, A.V. Chentsov, A.D. Bykov, M.V. Makarova, S.S. Voronina and F.C. Cruz, Spectra Chimica Acta A. (2024).

[26] B.A. Voronin, J. Tennyson, S.N. Yurchenko, T.Y. Chesnokova, A.V. Chentsov, A.D. Bykov, M.V. Makarova, S.S. Voronina and F.C. Cruz, Spectrochim. Acta. A Mol. Biomol. Spectrosc. **311**, 124007 (2024). doi:10.1016/j.saa.2024.124007

[27] M.J. Schueller, (Ed.) Investigating $H_2^{14}O$ and $^{10}CO_2$ as Cerebral Blood Flow Tracers in PET, University of Wisconsin–Madison, 2001.

[28] A. Serafini and J. Beaver, *Medical Cyclotrons in Nuclear Medicine. Progress in Nuclear Medicine* (Karger, 1978).

[29] F. Guo, *Nuclear Reactions with ^{11}C and ^{14}O Radioactive Ion Beams* (University of California, Berkeley, CA, 2004).

[30] D. Lee, *Study of Nuclear Reactions with ^{11}C and ^{15}O Radioactive Ion Beams (Nuclear Engineering)* (University of California, Berkeley, CA, 2007).

[31] F. Helus, *Radionuclides Production: Vol 2, Routledge Revivals* (CRC Press, 2019).

[32] J. Powell, J.P. O'Neil and J. Cerny, Production of an accelerated oxigen-14 beam, Lawrence Berkeley National Laboratory, EMIS-14 Abstract 86 (LBNL report N50223) (2002), pp. 1–9.

[33] D.W. Bardayan and M.S. Smith, Phys. Rev. C **56** (3), 1647–1650 (1997). doi:10.1103/PhysRevC.56.1647

[34] M. Wiescher, J. Görres and H. Schatz, J. Phys. G: Nucl. Part. Phys. **25** (6), R133–R161 (1999). doi:10.1088/0954-3899/25/6/201

[35] M. Dufour and P. Descouvemont, Nucl. Phys. A **730** (3-4), 316–328 (2004). doi:10.1016/j.nuclphysa.2003.11.012

[36] C.E. Fields, R. Farmer, I. Petermann, C. Iliadis and F.X. Timmes, Astrophys. J **823** (1), 46 (2016).

[37] A. Pichard, J. Mrazek, M. Assie, M. Hass, M. Honusek, G. Lhersonneau, F. Santos, M. Saint-Laurent and E. Simeckova, Eur. Phys. J. A **47** (6), 72 (2011). doi:10.1140/epja/i2011-11072-9.

[38] I.I. Bubukina, O.L. Polyansky, N.F. Zobov and S.N. Yurchenko, Opt. Spectrosc. **110** (2), 160–166 (2011). doi:10.1134/S0030400X11020032

[39] L. Lodi, J. Tennyson and O.L. Polyansky, J. Chem. Phys. **135** (3), 034113 (2011). doi:10.1063/1.3604934

[40] J. Tennyson, M.A. Kostin, P. Barletta, G.J. Harris, O.L. Polyansky, J. Ramanlal and N.F. Zobov, Comput. Phys. Commun. **163** (2), 85–116 (2004). doi:10.1016/j.cpc.2003.10.003

[41] O.L. Polyansky, A.G. Császár, S.V. Shirin, N.F. Zobov, P. Barletta, J. Tennyson, D.W. Schwenke and P.J. Knowles, Science **299** (5606), 539–542 (2003). doi:10.1126/science.1079558

[42] M. Wang, W.J. Huang, F.G. Kondev, G. Audi and S. Naimi, Chin. Phys C **45** (3), 030003 (2021). doi:10.1088/1674-1137/abddaf

[43] E.K. Conway, I.E. Gordon, A.A. Kyuberis, O.L. Polyansky, J. Tennyson and N.F. Zobov, J. Quant. Spectrosc. Radiat. Transf. **241**, 106711 (2020). doi:10.1016/j.jqsrt.2019.106711

[44] J. Tennyson, C. Hill and S.N. Yurchenko, Data structures for ExoMol: Molecular line lists for exoplanet and other atmospheres, in 6^{th} international conference on atomic and molecular data and their applications ICAMDATA-2012, Vol. 1545 of AIP Conference Proceedings, AIP, New York, 2013, pp. 186–195.

[45] P.R. Bunker and P. Jensen, *Molecular Symmetry and Spectroscopy* (2nd ed. NRC Research Press, Ottawa, 1998).

[46] J. Tennyson, S.N. Yurchenko, A.F. Al-Refaie, V.H.J. Clark, K.L. Chubb, E.K. Conway, A. Dewan, M.N. Gorman, C. Hill, A.E. Lynas-Gray, T. Mellor, L.K. McKemmish, A. Owens, O.L. Polyansky, M. Semenov, W. Somogyi, G. Tinetti, A. Upadhyay, I. Waldmann, Y. Wang, S. Wright and O.P. Yurchenko, J. Quant. Spectrosc. Radiat. Transf. **255**, 107228 (2020). doi:10.1016/j.jqsrt.2020.107228

[47] G. Box, G. Jenkins and G. Reinsel, *Time Series Analysis: Forecasting and Control, Wiley Series in Probability and Statistics* (Wiley, 2013).

[48] T. Furtenbacher, R. Tóbiás, J. Tennyson, O.L. Polyansky and A.G. Császár, J. Phys. Chem. Ref. Data **49** (3), 033101 (2020). doi:10.1063/5.0008253

[49] B.A. Voronin, Optika Atmosfery I Okeana **33** (11), 849–853 (2020).

[50] G.J. Harris, S. Viti, H.Y. Mussa and J. Tennyson, J. Chem. Phys. **109** (17), 7197–7204 (1998). doi:10.1063/1.477400

[51] M. Vidler and J. Tennyson, J. Chem. Phys. **113** (21), 9766–9771 (2000). doi:10.1063/1.1321769

[52] B.A. Voronin, N.N. Lavrentieva, T.P. Mishina, T.Y. Chesnokova, M.J. Barber and J. Tennyson, J. Quant. Spectrosc. Radiat. Transf. **111** (15), 2308–2314 (2010). doi:10.1016/j.jqsrt.2010.05.015

[53] L.S. Rothman, D. Jacquemart, A. Barbe, D.C. Benner, M. Birk, L.R. Brown, M.R. Carleer, C. Chackerian, K. Chance, L.H. Coudert, V. Dana, V.M. Devi, J.-M. Flaud, R.R. Gamache, A. Goldman, J.-M. Hartmann, K.W. Jucks, A.G. Maki, J.-Y. Mandin, S.T. Massie, J. Orphal, A. Perrin, C.P. Rinsland, M.A.H. Smith, J. Tennyson, R.N. Tolchenov, R.A. Toth, J. Vander Auwera, P. Varanasi and G. Wagner, J. Quant. Spectrosc. Radiat. Transf. **96** (2), 139–204 (2005). doi:10.1016/j.jqsrt.2004.10.008

[54] A.A. Mitsel, I. Ptashnik, K. Firsov and B. Fomin, Atmos Ocea. Opt. **8**, 847–850 (1995).

[55] E.J. Mlawer, V.H. Payne, J.-L. Moncet, J.S. Delamere, M.J. Alvarado and D.C. Tobin, Phys. Eng. Sci. **370** (1968), 2520–2556 (2012). doi:10.1098/rsta.2011.0295